Hyperspectral Fluorescence Imaging for Mouse Skin Tumor Detection

Seong G. Kong, Matthew E. Martin, and Tuan Vo-Dinh

This paper presents a hyperspectral imaging technique based on laser-induced fluorescence for non-invasive detection of tumorous tissue on mouse skin. Hyperspectral imaging sensors collect image data in a number of narrow, adjacent spectral bands. Such high-resolution measurement of spectral information reveals contiguous emission spectra at each image pixel useful for the characterization of constituent materials. The hyperspectral image data used in this study are fluorescence images of mouse skin consisting of 21 spectral bands in the visible spectrum of the wavelengths ranging from 440 nm to 640 nm. Fluorescence signal is measured with the use of laser excitation at 337 nm. An acousto-optic tunable filter (AOTF) is used to capture images at 10 nm intervals. All spectral band images are spatially registered with the reference band image at 490 nm to obtain exact pixel correspondences by compensating the spatial offsets caused by the refraction differences in AOTF at different wavelengths during the image capture procedure. The unique fluorescence spectral signatures demonstrate a good separation to differentiate malignant tumors from normal tissues for rapid detection of skin cancers without biopsy.

Keywords: Hyperspectral imaging, skin tumor detection, fluorescence, medical diagnostics, acousto-optic tunable filter.

Manuscript received Mar. 15, 2006; revised Aug. 23, 2006.

This research was supported by Computational Science Initiative of the University of Tennessee and the Oak Ridge National Laboratory. This work was also supported by funding from the National Institute of Health under grant number RO1 CA88787-01 and by the U.S. Department of Energy (DOE) Office of Chemical and Biological National Security and the DOE Office of Biological and Environmental Research, under contract DEAC05-000OR22725 with UT-Battelle.

Seong G. Kong (phone: + 1 865 974 3861, email: skong@utk.edu) is with Department of Electrical and Computer Engineering, The University of Tennessee, Knoxville, TN, USA.

Matthew E. Martin (email: martinme@ornl.gov) and Tuan Vo-Dinh (email: vodinht@ornl.gov) are with Life Science Division, Oak Ridge National Laboratory, Oak Ridge, TN, USA.

I. Introduction

Cancer is the second leading cause of death in the United States, exceeded only by cardiovascular diseases [1]. About one million new cancer cases are expected to be diagnosed and about a half million Americans die of cancer every year. These estimates do not include approximately 1.3 million cases of basal and squamous cell skin cancers that exist in the same time period. Cancers that develop from melanocytes, the pigment-producing cells of the skin, are called melanomas. Melanomas can spread quickly to other parts of the body through the lymph system or through the blood. For most skin cancer patients including melanoma and non-melanoma skin cancers, early diagnosis and thorough treatment such as complete resection are the keys to gaining a favorable prognosis.

Current diagnostic methods for skin cancers rely on physical examination of lesions in conjunction with skin biopsy, which involves the removal of tissue samples from the body for examination. Biopsy of large lesions often requires substantial tissue removal. Though this protocol for skin lesion diagnosis has been accepted as the gold standard, it is subjective, invasive, and time-consuming. Laboratory results for the determination of histopathology of a suspected tumor may generally take several days. Since suspicious areas are identified by visual inspection alone, there are a significant number of false positives that undergo biopsy. Conversely, many malignant lesions can also be overlooked. There is an urgent need for objective criteria that would aid the clinician in evaluating whether biopsy is required.

Optical techniques such as laser-induced fluorescence spectroscopy [2], [3] have been suggested as an effective tool in medical diagnostics. Spectroscopy offers an instant, non-

invasive diagnostic method to detect skin tumors, a typical symptom of skin cancer, based on the spectral properties of tissue [4], [5]. An optical device that combines fluorescence spectroscopy, white light diffuse reflectance spectroscopy, and video imaging has been developed for early detection of cervical cancers [6]. A three-dimensional volume of data in spatial and spectral space characterizes a hyperspectral image. A hyperspectral image contains spatial (x, y) information measured at a sequence of narrow-band wavelengths across a sufficiently broad spectral (z) range. Hyperspectral imaging sensors provide contiguous spectral signatures obtained from dozens or hundreds of narrow spectral channels. This enables hyperspectral imaging to reveal more useful information for material identification than conventional imaging techniques [7], [8]. Different tissues exhibit unique spectral characteristics of absorption and reflectance at particular bandwidths [9]. With high resolution and multiple spectral bands, subtle differences in the signature characteristics of tissues can be identified [10].

This paper presents a hyperspectral fluorescence imaging technique based on laser-induced fluorescence for non-invasive detection of tumorous tissue on mouse skin. Laser-induced fluorescence imaging techniques are generally regarded as sensitive optical tools and have proven to be useful in a number of scientific areas [10], [11]. Fluorescence is a phenomenon that begins when light is absorbed by a molecule at a given wavelength and concludes when that molecule emits light at a longer wavelength. The fluorescence imaging described in this paper involves excitation of fluorophores within a tissue medium by an external ultraviolet light source. Excitation with ultraviolet light results in the emission of fluorescence. There are a number of compounds that emit fluorescence in the visible spectral range when excited with ultraviolet radiation. The altered biochemical and morphological state of the neoplastic tissue is reflected in the spectral characteristics of the measured fluorescence. The spectral signatures of hyperspectral fluorescence imaging are compared to a traditional point spectroscopic analysis of the same mouse sample to validate the proposed method.

II. Hyperspectral Fluorescence Imaging for Skin Tumor Detection

1. Imaging System Setup

The Advanced Biomedical Science and Technology Group at Oak Ridge National Laboratory (ORNL) in Tennessee has developed advanced instrumentation for hyperspectral imaging of reflectance and fluorescence for a wide variety of applications including environmental sensing [12] and medical diagnostics [13], [14]. For this study, the hyperspectral imaging system has been further adapted for skin cancer diagnostics. Figure 1 shows a schematic diagram of hardware components of the ORNL hyperspectral imaging system used to obtain hyperspectral images. This system consists of fiber probes for image signal collection, an endoscope, an acousto-optic tunable filter (AOTF) for wavelength selection, a laser excitation source, an endoscopic illuminator (model Olympus CLV-10) equipped with a 300 watt CW Xe arc lamp source, a charge-coupled device (CCD) color camera (model Sony CCD-Iris) for reflectance detection, an intensified charge-coupled device (ICCD) camera (model IMAX-512-T-18 Gen. II) for fluorescence imaging, and a spectrometer for single point spectroscopic measurements.

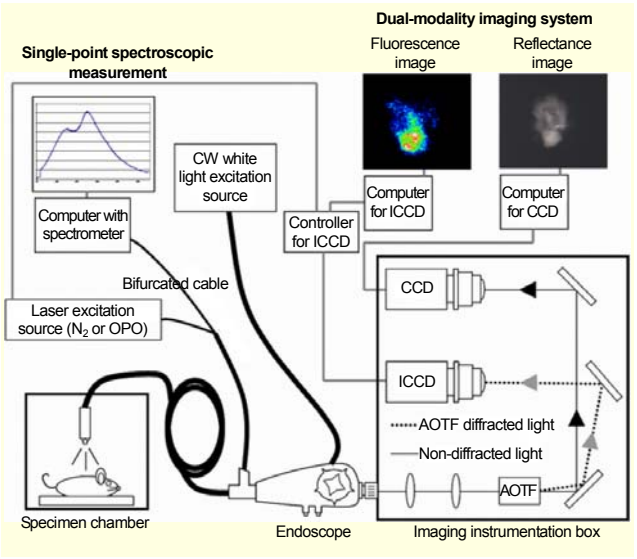

Fig. 1. Hardware components of the ORNL hyperspectral imaging system.

2. Hyperspectral Image Data Acquisition

Both fluorescent and reflected light are collected through the endoscope into the AOTF device via collimating lenses. A mirror placed in front of the AOTF projects the acquired images onto the ICCD camera for fluorescence imaging and onto the CCD camera for reflectance measurement. Excitation for the reflectance images is accomplished using an endoscopic illuminator. The reflectance light source was coupled to a gastrointestinal endoscope (Olympus T120) equipped with an imaging bundle. Excitation for the fluorescence spectra and images is accomplished using a LSI pulsed nitrogen laser (model VSL-337) with a maximum repetition rate of 20 Hz.

The fluorescent light emitted by the tissues is diffracted by the AOTF (Brimrose TEAF10-0.4-0.65-S) at a 6° angle from the undiffracted (zero-order) beam thus separating the reflected image from the fluorescent image. Individual wavelengths diffracted by the AOTF are thus sent to the ICCD. A Brimrose

AOTF controller (model VFI-160-80-DDS-A-C2) controls the AOTF. The controller sends a radio frequency (RF) signal to the AOTF based on input provided by the Brimrose software. Wavelength selection takes place in microseconds enabling ultra-fast modulation of wavelength output to the ICCD. Images of 21 spectral bands were taken in the visible spectrum region from 440 nm to 640 nm at every 10 nm spectral resolution.

Fluorescence images were acquired by gating the intensified ICCD camera. A timing generator incorporated into the ICCD camera's controller (ST-133) allowed the ICCD to operate in the pulsed mode with a wide range of programmable functions. A 500 ns delay between the laser trigger and the detector activation was programmed to synchronize the laser and the detector. The intensifier was gated for 500 ns during which a 5 ns laser pulse was delivered to the tissues. An image was captured 20 times per second, integrated by internal software, and output to a screen once per second. This allows real-time fluorescence detection. Single point spectroscopic measurements were taken to validate the experimental results. These measurements were taken at corresponding locations to the fluorescence imaging data. A compact fiber optic spectrometer (Ocean Optics USB2000), which covers the 360 to 1000 nm wavelength range, was used as the wavelength selection device instead of AOTF.

The hyperspectral image data used in this experiment are laser-induced fluorescence images taken from a mouse sample at ORNL. An adult mouse was injected subcutaneously with 100 μL of Fischer rat 344 rat tracheal carcinoma cells (IC-12) to induce tumor formation. A nude mouse was used to allow the implanted cancer cells to be able to grow due to the lack of an immune system in the animal. The lack of hair on the mouse enabled imaging directly without the need for depilation. The subdermal injection was done as close to the skin surface as possible to allow tumor formation close to the skin surface. This also allowed experiments to be performed *in vivo* rather than after tissue extraction. Experiments performed on whole animals are a vast improvement over those performed on tissue samples due to closer simulation of *in vivo* human cancerous conditions. After injection, the nude mouse was incubated for a period of four days to allow tumor formation to occur. Once a tumor was observed of approximately 1 cm, the mouse was anesthetized for approximately 30 minutes to permit data collection. After data collection, the mouse was humanely sacrificed to avoid undue suffering. The ORNL committee on the ethical treatment of animals acted as a governing body on all matters concerning animal testing and all work was done under Internal Animal Care and Use Committee (IACUC) #A3170-01. Strict protocols advised by the committee were followed when dealing with animals.

The measured hyperspectral fluorescence images consist of 165×172 pixels with 21 spectral bands from the wavelength λ_1 (440 nm) to λ_{21} (640 nm) at 10 nm spectral resolution in the spectral region. Such a high spectral resolution provides sufficient information for precise study of tumor detection. Figure 2(a) shows a reflectance image of a skin tumor region taken from a mouse sample. Figure 2(b) shows a fluorescence image of the sixth spectral band (490 nm) of the same tumor spot. The lower part of the fluorescence image (a bright U-shaped area) corresponds to normal tissue, while the dark area above the normal tissue reveals a tumor region as indicated in Fig. 5.

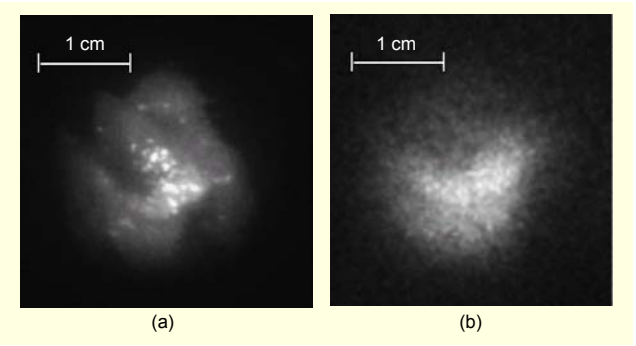

Fig. 2. Tumor region of a mouse skin sample. (a) Reflectance image and (b) fluorescence image at wavelength 490 nm.

3. Registration of Spectral Band Images

Original spectral band images captured by the hyperspectral imaging system are not spatially aligned since AOTF diffracts the light at different wavelengths [15], [16]. An AOTF is an optical bandpass filter whose passband can be electronically tunable using the acousto-optic interaction inside an optical medium whose refractive index is changed by an acoustic wave. Acousto-optics involves the interaction of sound and light in dielectric materials. When the sound propagates through a solid or liquid, compressions are created in the material that cause variable refraction of the passing light, pulling color features from it. Filters can be used to pass light with either a single wavelength or multiple wavelengths, depending on the RF signals applied generating acoustic waves. A piezoelectric oscillator bonded to an acousto-optic medium converts a high-frequency electrical signal into an ultrasonic wave. The AOTF allows the user to select and transmit a single wavelength from the incoming light. The acoustic wave produces a wavelength-selective single-tone grating in the AOTF transducer that can be varied by simply changing the acoustic frequency. The RF amplitude level applied to the transducer controls the filtered light intensity level. The AOTF has a dynamic range of 400 to 650 nm with a 10 mm ×10 mm aperture and a spectral resolution of 1 to 2 nm. The AOTF shows a fast response time (in μs), is accurate, and exhibits a high extinction ratio.

The AOTF produces spatial offset between neighboring spectral band images. Figure 3(a) shows the amount of offsets at different wavelengths that the AOTF generates during the image capturing procedure. The offsets are estimated by maximizing the mutual information between the given band images and the reference band image. The spectral band of the wavelength 490 nm was selected as a reference band with zero offset. A positive (negative) offset value indicates that the band image is shifted to the left (right) by the amount of pixels with respect to the reference band. Figure 3(b) illustrates that a spectral band image at 540 nm is spatially co-registered with the reference image at 490 nm after translating the 540 nm image to the left by the amount of offset (14 pixels).

All the spectral band images are spatially co-registered with the reference band image at 490 nm to obtain exact pixel-to-pixel correspondence by eliminating the offsets before extracting spectral signatures. Figure 4 shows eight sample spectral band images from wavelengths 450 nm to 590 nm after the registration discussed above. The reference spectral band at 490 nm gives the strongest response in terms of fluorescence intensity.

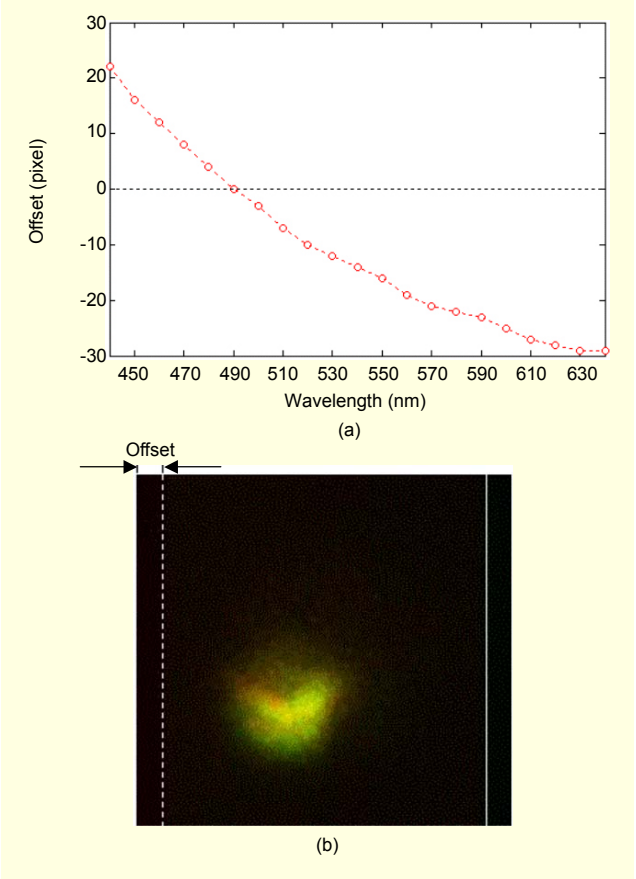

Fig. 3. (a) The amount of spatial offsets of spectral band images caused by the AOTF with respect to the reference band at 490 nm and (b) registered band images of 490 nm and 540 nm.

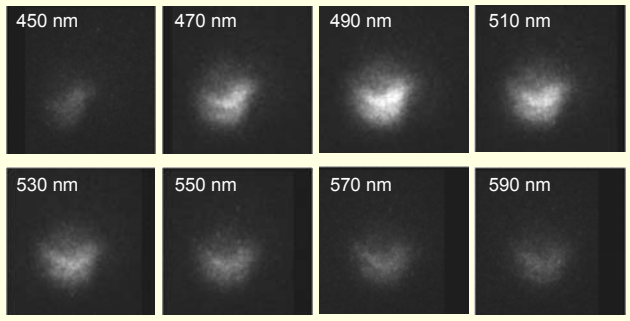

Fig. 4. Spectral band images from the wavelengths of 450 nm to 590 nm.

III. Spectral Characteristics of Normal Tissue and Malignant Tumor

Experiments with a mouse sample having a tumor region provide an illustration of the potential of the proposed hyperspectral fluorescence imaging technique for *in vivo* skin cancer diagnosis. Optical imaging of reflectance demonstrates nearly uniform responses to both normal tissue and skin tumor areas, which makes visual classification of malignant tumors difficult based on reflectance images. Figure 5 visualizes a mosaic of reflectance image and fluorescence image at the wavelength of 490 nm. A mouse tumor expert at ORNL verified the tumor location on the mouse skin. Fluorescence shows better discrimination for a skin tumor region. The fluorescence component shows a stronger response to normal tissue in comparison to the tumor region. Normal tissue corresponds to the bright U-shaped area with stronger fluorescence intensity. The relatively darker area in fluorescence intensity marked by a circle above normal tissue indicates a malignant tumor region.

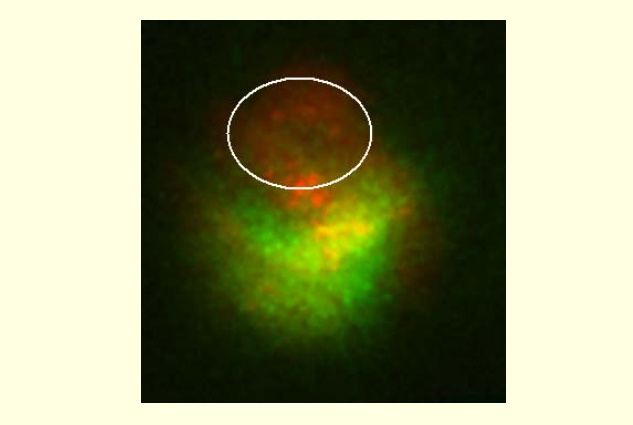

Fig. 5. Mosaic of fluorescence and reflectance images. A circular region was identified as a malignant tumor by a tumor expert. Fluorescence intensity of the tumor region shows weaker response than that of normal tissue.

Hyperspectral image data can be represented by a three-dimensional (3-D) cube of data I(m, n, λ_i), where (m, n) denotes the spatial coordinates of a pixel location in the image and λ_i denotes a spectral band (i = 1, 2,⋯, L), where L is the number of spectral bands (L = 21). Each pixel in the hyperspectral image can be represented as a spectral signature vector x=(x_1,⋯, x_L), where x_i denotes an i-th spectral component. For hyperspectral fluorescence measurements, the choice of the laser excitation wavelength is important. In this study, an N_2-pumped laser at wavelength 337 nm was used as an excitation source of the fluorescence signal. A nitrogen laser provides the lowest excitation wavelength of 337 nm that corresponds to the highest energy. Longer wavelengths can be selected for excitation by using the tunable dye laser system. However, the use of shorter wavelengths tends to excite more components in tissues. This wavelength produces fluorescence spectra of spectral signatures useful to discriminate between normal and malignant tissues.

Figure 6 shows fluorescence spectra taken from a mouse sample in terms of two categories of interest: normal tissue and malignant tumor. The spectral signatures show a peak response near the wavelength 490 nm while the fluorescence intensity of malignant tumor is weaker than that of the normal tissue. The higher fluorescence intensities in the normal tissue can be attributed to several factors, depending on what collection wavelength region is being described. In the wavelength region of 450 nm to 510 nm, the higher fluorescence intensity seen in the normal tissues is due primarily to a decrease in collagen and elastin from normal to malignant tissues and a decrease in nicotinamide adenine dinucleotide (NADH) levels in the malignant tissues. The decreases in fluorescence seen in the images in the wavelength region between 500 nm and 600 nm can be attributed to the whole blood absorption in this region

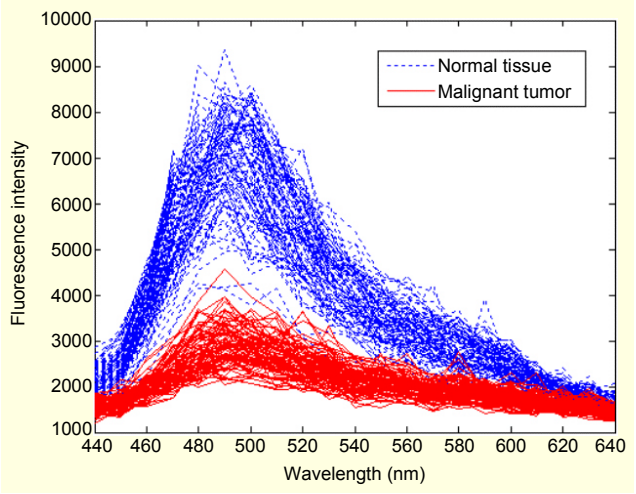

Fig. 6. Spectral signature of normal tissue and malignant tumor. The fluorescence intensity is measured with a laser excitation at wavelength 337 nm.

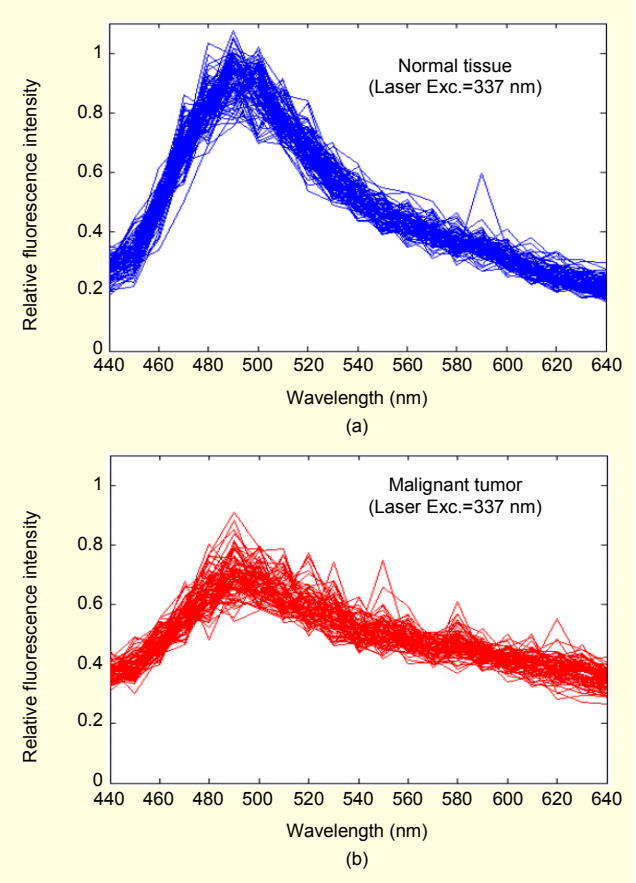

Fig. 7. Fluorescence spectra normalized with respect to the area under the spectral curve. (a) Normal tissue and (b) malignant tumor.

[17]. An increase in blood volume in the malignant tissues causes more of the fluorescence from fluorophores such as lipo-pigments and flavins to be absorbed.

The intensity of the fluorescence signal may not be a consistent parameter according to several factors such as blood flow, hemoglobin absorption, and surface morphology. The distance between the tissue surface and probe can also affect the intensity of recorded fluorescence signal. Spectral profiling reveals more consistent tissue characteristics. Figure 7 illustrates the spectral signature curves of normal tissue and malignant tumor normalized with respect to the area under the curve. The normalization procedure significantly reduced the within-class variances. The spectral signatures after normalization demonstrate a good separation to differentiate malignant tumors from normal tissues.

To compare the spectral signature curves of Fig. 7 to a traditional point spectroscopic analysis, point spectroscopic measurements were taken from the same mouse and are shown in Fig. 8. We made 559 measurements of fluorescence intensity for each curve from 440 nm to 640 nm at a 0.36 nm interval. Notice the similarity between the normal and malignant

spectral signature curves of Fig. 7 and the point spectroscopic curves of Fig. 8. A peak in the normal and malignant spectral signature data is observed around 490 nm in Fig. 7 and is confirmed by the point spectroscopic data of Fig. 8. This agreement in spectral information lends credence to our imaging system's capability of spectral discrimination.

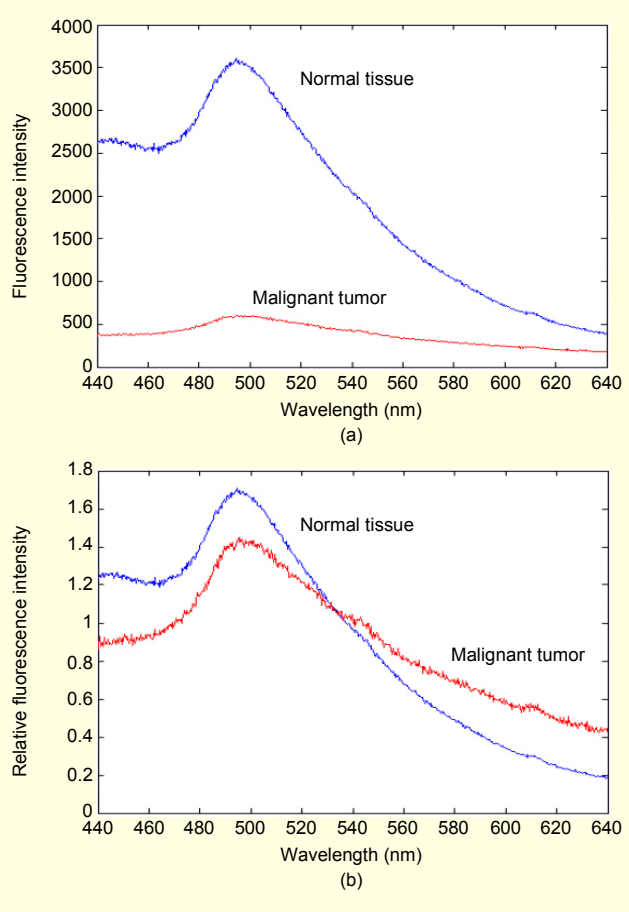

Fig. 8. Point spectroscopic measurements of the mouse tissue sample. (a) Raw data and (b) normalized spectral signatures with respect to the area under the curve.

IV. Conclusions

This paper presents a hyperspectral fluorescence imaging technique for non-invasive detection of malignant tumors on mouse skin. Skin tumors are often not as visually obvious as other pathological diseases since their signature appears as shape distortion rather than discoloration. This makes tumor detection difficult based on reflectance images. Hyperspectral fluorescence imaging reveals high-resolution spectral information useful for the classification of malignant skin tumors. Fluorescence data captured by the hyperspectral imaging system involves a higher level of contrast and thus provides a greater possibility of detecting tumors. Hyperspectral images generated by acousto-optic tunable filters typically demonstrate spatial offsets between the band images. The offsets are estimated using the mutual information of the given band and the reference band image at 490 nm. All the band images are spatially registered to obtain exact pixel correspondences by compensating the offsets. Raw spectral signatures measured from a mouse sample are normalized with respect to the area under the curve. Normalized fluorescence intensities significantly reduce the within-class variances and demonstrate distinguishable features of relative intensity differences to discriminate malignant tumors from normal tissues. For example, the ratios of the peak intensities at 490 nm and 440 nm are 0.4 for tumor and 0.8 for normal tissue, twice as much as the tumor case. This data was corroborated with point spectroscopic measurements. The proposed hyperspectral fluorescence imaging technique can lead to the development of non-invasive *in vivo* detection of skin cancer without the need of tissue biopsy.

References

[1] *Cancer Facts and Figures*, American Cancer Society, 2002.

[2] A.R. Tumlinson, L.P. Hariri, U. Utzinger, and J.K. Barton, "Miniature Endoscope for Simultaneous Optical Coherence Tomography and Laser-Induced Fluorescence Measurement," *Applied Optics*, vol. 43, no. 1, 2004, pp. 113-121.

[3] T. Vo-Dinh, M. Panjehpour, B.F. Overholt, and P. Buckley III, "Laser-Induced Differential Fluorescence for Cancer Diagnosis without Biopsy," *Applied Spectroscopy*, vol. 51, no. 1, 1997, pp. 58-63.

[4] J. Zhang, C. Chang, S. Miller, and K. Kang, "Optical Biopsy of Skin Tumors," *Proc. 21st Annual Conf. Engineering in Medicine and Biology*, vol. 2, Oct. 1999, p.1095.

[5] K. Chao, P. Mehl, and Y. R. Chen, "Use of Hyper- and Multi-Spectral Imaging for Detection of Chicken Skin Tumors," *Applied Engineering in Agriculture*, vol. 18, no. 1, 2002, pp. 113-119.

[6] MediSpectra Inc., http://www.medispectra.com/news/news.html, 2006.

[7] G. Shaw and D. Manolakis, "Signal Processing for Hyperspectral Image Exploitation," *IEEE Signal Processing Magazine*, vol. 19, no. 1, Jan. 2002, pp. 12-16.

[8] D. Landgrebe, "Hyperspectral Image Data Analysis as a High Dimensional Signal Processing Problem," *IEEE Signal Processing Magazine*, vol. 19, no. 1, 2002, pp. 17-28.

[9] C. Chang, Q. Du, T. Sun, and M. Althouse, "A Joint Band Prioritization and Band-Decorrelation Approach to Band Selection for Hyperspectral Image Classification," *IEEE Trans. Geoscience and Remote Sensing*, vol. 37, no. 6, Nov. 1999, pp. 2631-2641.

[10] S.G. Kong, Y.R. Chen, I. Kim, and M.S. Kim, "Analysis of Hyperspectral Fluorescence Images for Poultry Skin Tumor Inspection," *Applied Optics*, vol. 43, no. 4, Feb. 2004, pp. 824-833.

[11] B. Albers, J. DiBenedetto, S. Lutz, and C. Purdy, "More Efficient

Environmental Monitoring with Laser-Induced Fluorescence Imaging," *Biophotonics Int'l Magazine,* vol. 2, no. 6, Nov. 1995, pp. 42-54.

[12] S.M. Moreau, D.M. Hueber, and T. Vo-Dinh, "Fiber-Optic Remote Multisensor System Based on an Acousto-Optic Tunable Filter (AOTF)," *Applied Spectroscopy*, vol. 50, no. 10, 1996, pp. 1295-1300.

[13] T. Vo-Dinh, D. L. Stokes, M. Wabuyele, M. E. Martin, J. M. Song, R. Jagannathan, E. Michaud, R.J. Lee, and X. Pan "A Hyperspectral Imaging System for In Vivo Optical Diagnostics," *IEEE Engineering in Medicine and Biology Magazine*, vol. 23, no. 5, 2004, pp. 40-49.

[14] M.E. Martin, M. Wabuyele, M. Panjehpour, B.F. Overholt, R. Denovo, S. Kennel, G. Cunningham, and T. Vo-Dinh "An AOTF-Based Dual-modality Hyperspectral Imaging System (DMHSI) Capable of Simultaneous Fluorescence and Reflectance Imaging," *Medical Engineering and Physics*, vol. 28, no. 2, 2005, pp. 149-155.

[15] N. Gupta and R. Dahmani, "Multispectral and Hyperspectral Imaging with AOTF for Object Recognition," *Proc. SPIE*, vol. 3584, 1999, pp. 128-135.

[16] I.-C. Chang, "Electronically Tuned Imaging Spectrometer Using an Acousto-Optic Tunable Filter," *Proc. SPIE*, vol. 1703, 1992, pp. 24-29.

[17] N. Bashkatov, E.A. Genina, V.I. Kochubey, and V.V. Tachin, "Optical Properties of Human Skin, Subcutaneous and Mucous Tissues in the Wavelength Range from 400 to 2000 nm," *J. Phys. D: Appl. Phys.*, vol. 38, no. 15, 2005, pp. 2543-2555.

Seong G. Kong received the BS and the MS degrees in electrical engineering from Seoul National University, Seoul, Korea in 1982 and 1987, respectively. He received the PhD degree in electrical Engineering from University of Southern California, Los Angeles, California in 1991. From 1992 to 2000, he was with the Department of Electrical Engineering at Soongsil University, Seoul, Korea as an Associate Professor. He was chair of the department from 1998 to 2000. Currently he is an Associate Professor of Electrical and Computer Engineering at the University of Tennessee, Knoxville. Dr. Kong was Editor-in-Chief of *Journal of Fuzzy Logic and Intelligent Systems* from 1996 to 1999. He is an Associate Editor of *IEEE Transactions on Neural Networks*. Dr. Kong received the Award for Academic Excellence from Korea Fuzzy Logic and Intelligent Systems Society in 2000. He received the Professional Development Award from the University of Tennessee in 2004, the Best Paper Award from IEEE International Workshop on Object Tracking and Classification beyond the Visible Spectrum, and a Paper Award from the American Society of Agricultural and Biological Engineers in 2005. He is a senior member of IEEE. Dr. Kong has authored more than 70 refereed journal articles, conference papers, and book chapters in the areas of image processing, pattern recognition, and intelligent systems.

Matthew E. Martin received the Bachelor of Science degree in mechanical engineering from Tennessee Technological University, Cookeville, TN, in 1998, and subsequently received the Master of Science degree in mechanical engineering from Tennessee Technological University in 2000. His thesis topic was "Microscopic Thermal Detector Optimization through Material and Geometric Selection." He then went to work for Haleos, Inc., a start-up firm in Blacksburg, VA that designed and built novel fiber optic subcomponents and MEMS devices. He entered Tennessee Technological University in the fall of 2002 and was awarded the Doctor of Philosophy Degree in engineering in 2005. His research topic was titled "Development of a Dual-modality Hyperspectral Imaging System (DMHSI) for the Detection of Esophageal Cancer." He is currently working as a Senior R&D Scientist for Siemens Molecular Imaging in Knoxville, TN.

Tuan Vo-Dinh is currently the Director of the Fitzpatrick Institute for Photonics and Professor of Biomedical Engineering and Chemistry at Duke University. Before joining Duke University in 2006, Dr. Vo-Dinh was a Group Leader of the Advanced Biomedical Science and Technology Group, and Director of the Center for Advanced Biomedical Photonics, and a Corporate Fellow, one of the highest honors for distinguished scientists at the Oak Ridge National Laboratory, Oak Ridge, Tennessee, USA. His research interests focus on the development of advanced technologies for human health protection and environmental sensing. His research activities involve biophotonics, nanophotonics, medical diagnostics, molecular imaging, laser spectroscopy, biophotonics, biosensors, nanosensors, and biochips. Dr. Vo-Dinh has authored over 350 publications in peer-reviewed scientific journals, is the author and editor of 7 books, and holds over 32 U.S. patents, six of which have been licensed to private companies for commercial development. Dr. Vo-Dinh is Editor-in-chief of *NanoBiotechnology* and Associate Editor of the *Journal of Nanophotonics*, *Plasmonics*, and *Environmental Toxicology*. Dr. Vo-Dinh has received numerous awards including seven *R&D 100 Awards* for Most Technologically Significant Advance in Research and Development for his pioneering research and inventions of innovative technologies.